

# Development and Characterization of In-situ Aluminum–Titanium Carbide Composites Prepared by Pneumatic Powder Injection Route

Sheetal Gupta, Anirban Giri, Saikat Adhikari and Vivek Srivastava

**Abstract** High costs, consistency and scalability are the major challenges in development of metal matrix composites. To overcome these challenges, a novel process has been demonstrated in which pneumatic powder injection was used instead of the conventional mechanical stirring process. In this study, aluminum–titanium carbide particulate composites were prepared in situ by injection of mixed salt of titanium ( $K_2TiF_6$ -potassium titanium fluoride salt) and graphite powder through submerged lance into molten aluminum. Uniform distribution of equiaxed  $Al_3Ti$  (aluminum–titanium intermetallic) particles and TiC (titanium carbide) particles were achieved depending on the reaction temperature and holding time. SEM-EDS confirmed the presence of submicron TiC particles distributed throughout the matrix. TiC particles generated in situ are thermodynamically more stable and tend to have cleaner matrix particle interfaces. More than 15% improvement in elastic modulus along with significant improvement in other mechanical properties was achieved by up to 10 wt% TiC reinforcement.

**Keywords** Metal matrix composites · In-situ · Pneumatic powder injection  
Modulus · TiC

## Introduction

In recent times, aluminum alloys have been gaining widespread acceptance in the automotive industry [1]. Conventional wrought aluminum alloys, however, have limitations with maximum achievable modulus and fatigue, creep and wear resistance. As high-performance lightweight materials, aluminum matrix composites (AMCs) reinforced with harder and stiffer ceramic particles are widely used in

---

S. Gupta (✉) · A. Giri · S. Adhikari  
Aditya Birla Science and Technology Company Private Limited, Navi Mumbai, India  
e-mail: sheetal.gupta@adityabirla.com

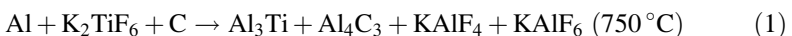
V. Srivastava  
Hindalco Industries Limited, Mumbai, India

aerospace, aircraft and automotive applications because of their excellent properties, such as high specific stiffness, high specific strength and excellent wear resistance [2]. Mass production of such materials of consistent quality and low cost, though, remains a challenge [3].

AMC manufacturing routes can be broadly classified as *ex situ* and *in-situ*. When the reinforcement is externally added to the matrix, *ex situ* composite materials are created. *In situ* synthesizing of metal matrix composites involves the production of reinforcements within the matrix during the fabrication process. *Ex situ* processes can be further sub-divided as either solid or liquid state process, though some gaseous state processes too have been reported in literature [4]. In brief, powder metallurgical (P/M) processes utilizes metal and reinforcement powders as the starting raw materials that are blended and consolidated to produce the composite. P/M route makes it possible to employ lower operating temperatures, overcome issues with particle wetting, minimize undesirable interfacial reactions and improve mechanical properties. Also, significantly higher reinforcement volume fractions can be incorporated through this route. P/M route, however, remains expensive compared to liquid metallurgy route, have higher levels of porosity and is suitable only for low volume manufacturing [5]. Liquid metallurgical processes for AMC synthesis include liquid infiltration, squeeze casting, spray co-deposition, stir casting and *in-situ* (reactive) processing.

The selection of the processing route depends on many factors including type and level of reinforcement loading and the degree of micro structural integrity desired [6]. For *ex situ* liquid metallurgical processes, lack of wetting of the reinforcement and interfacial reactions leading to poor interfacial bonding are major concerns. *In-situ* AMCs overcome these limitations but control of process variables remains an issue. Several liquid metallurgical process for *in-situ* production of particulate AMC have been reported in literature [7]. For these processes, kinetics of particle formation is not yet clear. The reaction rate depends on several factors like temperature, amount of stirring and presence of alloying elements etc.

There are several ceramic reinforcements available for Al-based metal matrix composites but in this study TiC has been considered due to its high hardness, stiffness and wear resistance properties [8–11]. These features of the TiC phase are combined in Al–TiC composites with the ductility, toughness, electrical and thermal conductivity of the aluminum matrix. Al–TiC composites can also potentially be used as grain refiner for aluminum alloys. TiC particles generated *in-situ* are also thermodynamically more stable, tend to have cleaner matrix–particle interfaces and are free from adsorbed gases, oxide films and detrimental reaction products. Aluminum matrix TiC composites have been reported earlier [2]. The following reaction sequence is reported for flux assisted synthesis of Al–TiC composite.



$K_2TiF_6$  and graphite react with molten aluminum at 750 °C (Reaction 1), where Ti is released from  $K_2TiF_6$  and dissolved in the melt, forming  $Al_3Ti$  whereas graphite reacts with Al and forms  $Al_4C_3$  particles. K–Al–F salt is also formed, which helps in cleaning the particle surfaces and remove the oxide layer from the surface of the melt.  $Al_3Ti$  and  $Al_4C_3$  particles react above 900 °C to form TiC particles which are more stable than  $Al_3Ti$  particles (Reaction 2).

The present work was undertaken to synthesize Al–TiC composites in situ by reacting  $K_2TiF_6$  and graphite in molten aluminum. The reactions involved in the synthesis were investigated by metallographic analysis of melt samples taken during the process.

## Experimental Procedures

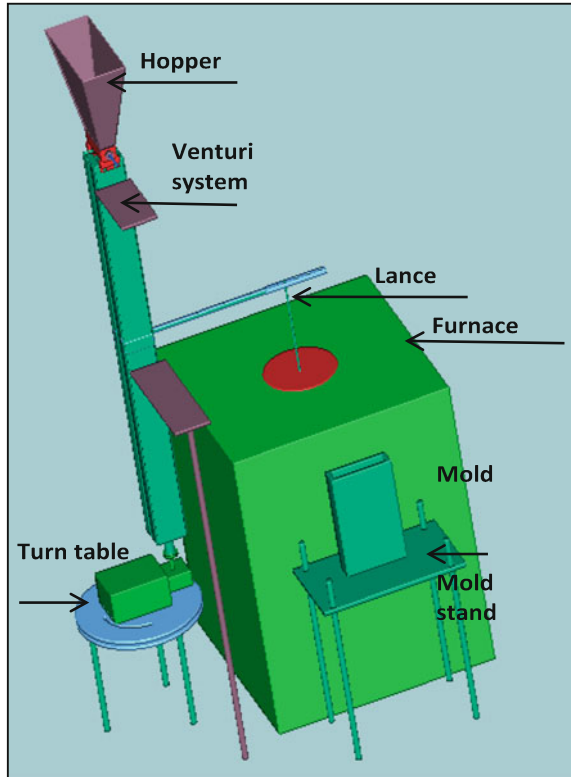
Particulate aluminum matrix composites (AMCs) from 0 to 10 wt% titanium carbide (TiC) reinforcement were prepared for this study using a modified salt flux assisted synthesis process.

Figure 1 shows the schematic experimental set up used for this study in which a 50 KW induction furnace with a 25 kg capacity silicon carbide crucible was employed. For powder injection, a powder hopper of 15 kg capacity, a venturi system and a lance assembly system was used. During synthesis, it was required to manipulate the lance assembly on (a) vertical axis to submerge the lance inside the molten metal and (b) horizontal axis during pouring the molten metal into the moulds. In order to facilitate these manipulations, the lance assembly was mounted on a screw-driven manipulator and a worm gear was placed between the steel channels of the mounting structure. A mating travelling gear moves on the vertical axis when the worm gear is operated. The lance assembly was attached to the travelling gear allowing the motion of the lance. This entire assembly itself was mounted on a turn table to enable movement of the lance assembly in horizontal direction through a swivel motion.

During synthesis, 15–20 kg commercial purity aluminum (99.5%) ingots were melted in an induction furnace at 800–900 °C. Graphite powder and  $K_2TiF_6$  salts were premixed as required by stoichiometry and injected into the melt through specially designed alumina or graphite lance to avoid thermal shock and lance chocking. The flux and graphite powders were injected at room temperature and no preheating was required.

During pneumatic powder injection, argon or nitrogen was used as a carrier gas to agitate the melt and prevent lance chocking. After completing the injection of the powders, the melt was held for 30–60 min at the reaction temperature to allow the reaction to proceed to completion while continuing gas bubbling to ensure mixing. At the end of the hold time, spent salt and dross was skimmed and the composite was poured in the molds to cast MMC ingots.

**Fig. 1** Schematic illustration of the experimental set up used for metal matrix composite synthesis



The pouring temperature was controlled by the induction furnace to obtain different reinforcement morphology. Multiple samples were taken from the cast ingot for microstructure and hardness measurements. Vickers hardness of the specimens was measured at 5 kgf load with dwell time of 10 s. For measuring the tensile properties of the composite specimens, the cast samples were machined to standard tensile specimens according to ASTM: B557M-10 standard and tested. The stress–strain data were recorded by using video extensometer attached with the tensile testing machine (model Zwick-Z050) according to the load–displacement data.

## Results and Discussion

Characterization of the cast composite samples was conducted to understand the formation of phases, their distribution within the composite and their effect on mechanical properties.

## Optical Microstructure

Figure 2a, b show microstructures of 5 wt% TiC as-cast composites at low magnification. Figure 2a shows the presence of 20–50  $\mu\text{m}$  sized blocky particles of  $\text{Al}_3\text{Ti}$  (confirmed by EDS) along with some residual graphite particles. Due to insufficient cleaning of the dross some of the carbon residue carried over from the melt which may affect the mechanical properties of the composite material. Figure 2b shows the SEM image of the 5 wt% TiC as-cast sample. Uniform distribution of blocky and needle shaped particles of  $\text{Al}_3\text{Ti}$  were observed throughout the matrix. TiC particles were not observed at lower magnifications. However, a distribution of sub-micron sized TiC particles was clearly identified at higher magnifications as seen in the SEM micrograph in Fig. 2c and EDS spectra in Fig. 2d. The clear majority of the  $\text{Al}_3\text{Ti}$  particles which formed at 750  $^\circ\text{C}$  were of blocky morphology as seen in Fig. 2a, b. Submicron TiC particles were formed at 900–950  $^\circ\text{C}$  after reacting of  $\text{Al}_3\text{Ti}$  particles with  $\text{Al}_4\text{C}_3$  particles. This is in agreement with the reaction mechanism described earlier for in-situ formation of TiC in aluminum melts and reported in literature [2].

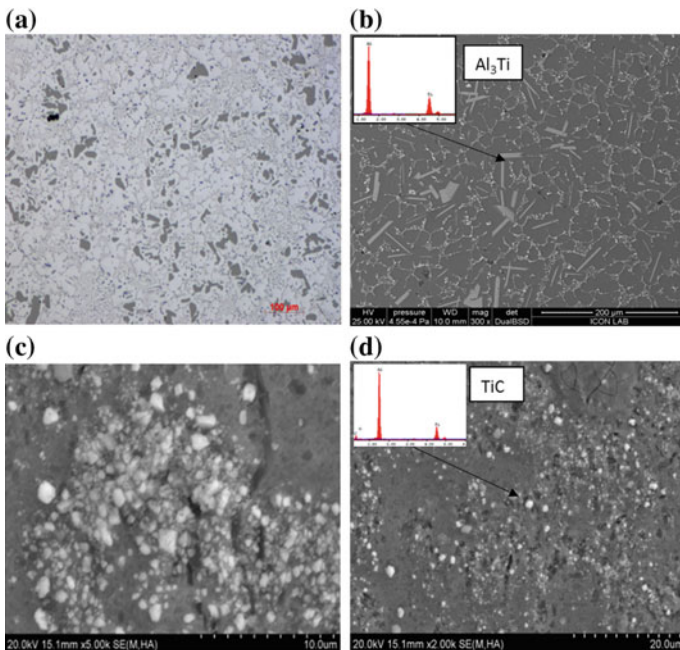


**Fig. 2** Microstructure of Al-5 wt% TiC composites: **a** Low magnification image of the composites having large blocky particles of  $\text{Al}_3\text{Ti}$  and some residual graphite particles **b** SEM image of needles shape of  $\text{Al}_3\text{Ti}$  particles **c** Distribution of fine sub-micron sized TiC particles **d** SEM-EDS image of submicron sized TiC particles

## *X-Ray Diffraction*

The microstructural investigations were confirmed by the XRD analysis, which revealed  $\text{Al}_3\text{Ti}$  and TiC reflections in aluminum matrix. Figure 3a shows the XRD pattern for two Al-5 wt%TiC composites prepared separately at 900 and 950 °C. The XRD pattern shows that maximum transformation of  $\text{Al}_3\text{Ti}$  to TiC could be achieved around 950 °C by the pneumatic powder injection process. Higher temperature favors the conversion of  $\text{Al}_3\text{Ti}$  particles to TiC particles. Figure 3b shows XRD pattern for different amount of reinforcement addition starting from 0 to 10 wt%, which clearly indicates increasing peak intensities of TiC with increasing amount of reinforcement addition.

## *Homogeneity and Consistency*

During synthesis, homogeneity and consistency of the different phases in the matrix are very important to achieve desired mechanical and surface properties. These can

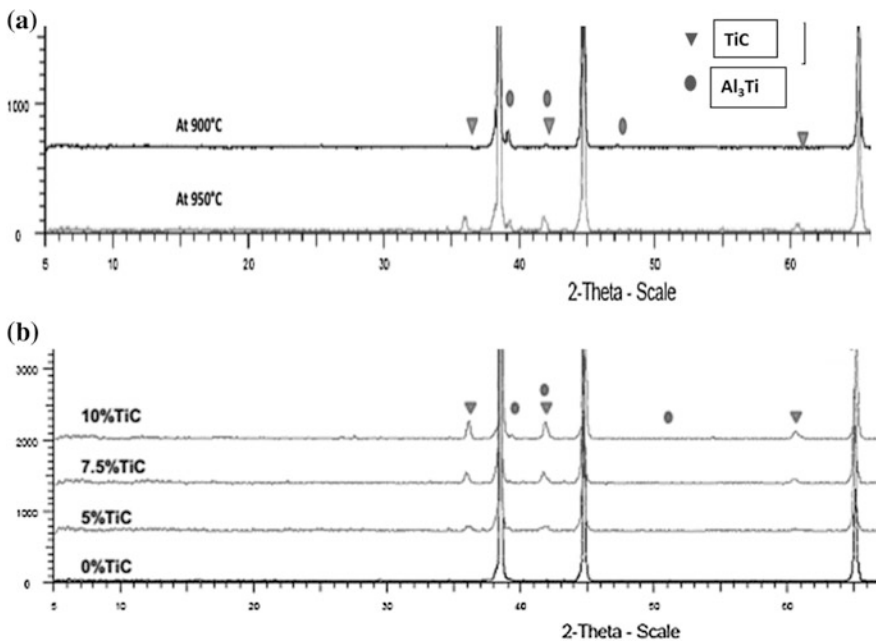
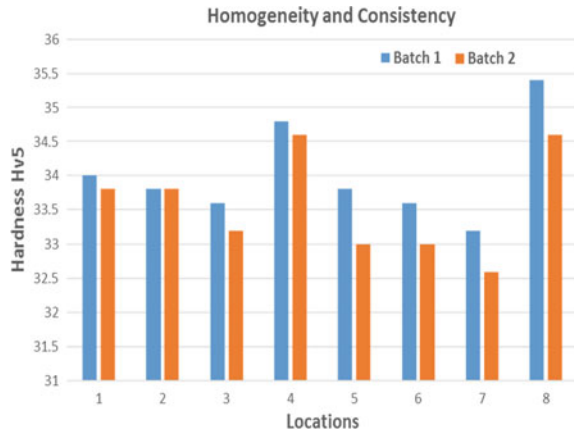


**Fig. 3** XRD pattern for Al-TiC composites **a** XRD pattern showing formation of TiC at increasing reaction temperature **b** increasing peak intensities of reinforcing species for different amount of reinforcement addition

**Fig. 4** Macro hardness of 5 wt% TiC composite at different locations and different batches



be analyzed by hardness measurement at different locations of the ingot from different batches. Figure 4 shows the effectiveness of the current synthesis route in consistently producing homogenous MMC material of 5 wt% TiC reinforcement. The homogeneity is achieved due to pneumatic injection of powder through a specially designed lance into the melt where argon or nitrogen were being used as a carrier gas. This process helps in agitating and mixing the powder uniformly throughout the melt to produce a fairly uniform macro-distribution of reinforcement particles which resulted in a  $\pm 3.0\%$  variation in macro-hardness within one batch and only  $\pm 1.1\%$  batch to batch variation.

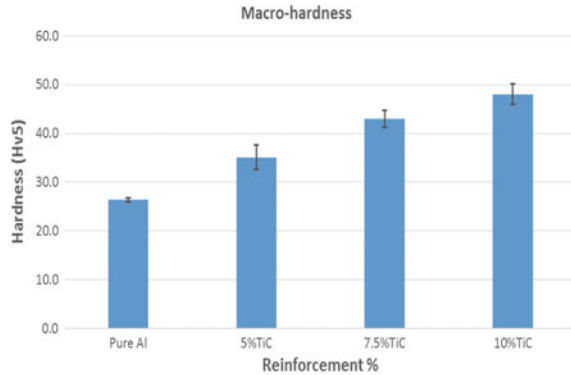
### ***Mechanical Properties***

To understand the effect of hard TiC and  $Al_3Ti$  particles on overall mechanical properties, hardness, tensile and young's modulus properties were measured.

#### **Macro-Hardness**

Figure 5 shows the macro-hardness values for the MMC material with 0–10 wt% TiC reinforcement. All values of hardness are the average for  $\sim 5$  samples from different batches. Figure 5 indicates that hardness values increase almost linearly with increasing TiC reinforcement. 5 wt% TiC reinforcement leads to 33% improvement in hardness over base alloy. Similarly, 7.5 and 10 wt% TiC reinforcement lead to 44 and 79% improvement in hardness respectively. These improvements in the hardness values are due to the addition of harder phases of TiC and  $Al_3Ti$ .

**Fig. 5** Macro-hardness of 0–10 wt% TiC reinforcement composite materials



### Tensile Properties

In the case of composites, reinforcements play a role in both the elastic and plastic regime. In the elastic regime, modulus of the composite is altered due to load transfer from the matrix to the composite. In the plastic regime, the deformation is primarily controlled by motion of dislocations in the matrix. Large reinforcement particles are mostly ineffective in restricting dislocation motion but do act as stress concentrators, thereby reducing the ductility of the composite. Finer particles, on the other hand, restrict dislocation motion, increase yield and tensile strength without severely compromising the ductility. In view of the above understanding, tensile properties were evaluated of 0–10 wt% TiC reinforcement composite materials.

The variation of yield strength, UTS and elongation values with TiC reinforcement are shown in Figs. 6, 7 and 8 respectively. Figures 6 and 7 clearly indicate that there is a marked increase in yield strength and UTS with increasing amount of TiC addition. Ductility of the composites as characterized by % elongation was found to be decrease with increasing reinforcement as seen in Fig. 8.

**Fig. 6** Yield strength of 0–10 wt% TiC reinforcement composite materials

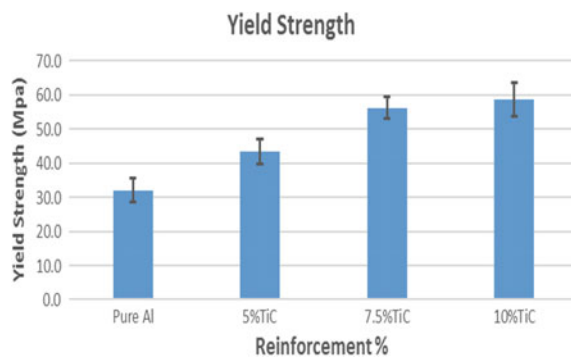




**Fig. 7** Ultimate tensile strength of 0–10 wt% TiC reinforcement composite materials

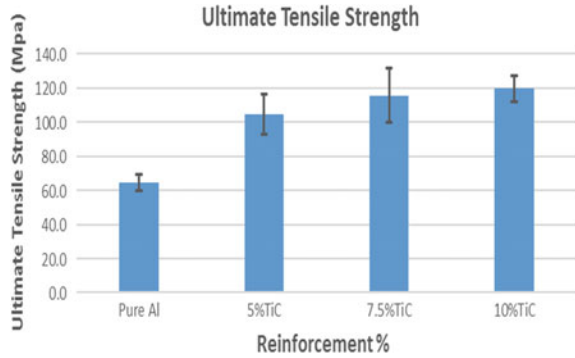


**Fig. 8** Elongation of 0–10 wt% TiC reinforcement composite materials

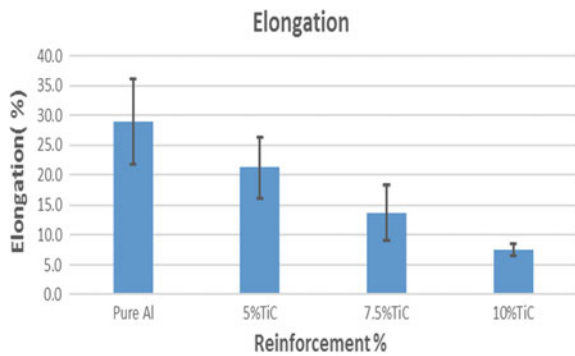
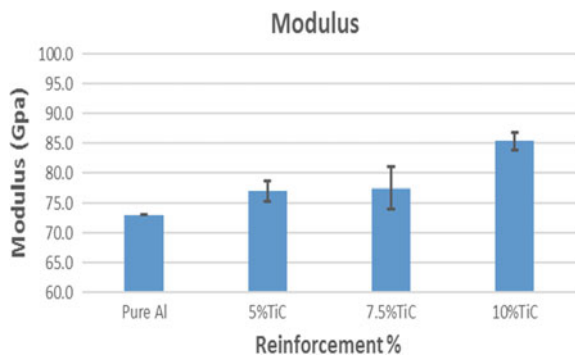


Figure 9 shows dependence of elastic modulus of the composites with TiC reinforcement. The elastic modulus increases with an increasing amount of TiC addition. This is due to the reinforcements being able to partially carry the applied load and reduce the actual stresses in the matrix. This also demonstrates the superior interfacial bonding of the reinforcement to the matrix. There was about 15% improvement in observed for 10 wt% TiC reinforcement as compared to the base alloy.

**Fig. 9** Modulus of 0–10 wt% TiC reinforcement composite materials



## Conclusions

1. At low reaction temperatures (750 °C), the composite contains only blocky  $\text{Al}_3\text{Ti}$  phases, which transforms to TiC as reaction temperature increases to 950 °C.
2. Volume fraction of  $\text{Al}_3\text{Ti}$  and TiC particles in Al–TiC composites increases with increasing  $\text{K}_2\text{TiF}_6$  and graphite powder addition into the aluminum melt.
3. Macro-hardness variation within one batch was  $\pm 3.0\%$  and batch to batch variation was  $\pm 1.1\%$ . The novel pneumatic injection method helped in agitating and mixing the powder throughout the melt leading to homogenous properties in the composite material.
4. Mechanical properties like hardness, yield strength and tensile strength improved almost linearly with amount of TiC addition in the aluminum matrix.
5. Ductility of the composite showed linearly decreasing trend with increasing amount of TiC addition.
6. Young's modulus also improved significantly with amount of TiC addition. For 10 wt% TiC reinforcement composite materials, the young's modulus increased by 15% as compared to the base alloy.

## References

1. Report on The road ahead-automotive materials. Ducker Worldwide Research Company 2016
2. Birol Y (2008) In situ synthesis of Al–TiC<sub>p</sub> composites by reacting  $\text{K}_2\text{TiF}_6$  and particulate graphite in molten aluminum. *J Alloy Compd* 454:110–117
3. Chawla KK (1998) Metal matrix composites. In: *Composite materials*. Springer, New York
4. Borgonovo C, Apelian D (2011) Manufacture of aluminum nanocomposites: a critical review. *Mater Sci Forum* 678:1–22
5. Liu YB, Lim SC, Lu L, Lai MO (1994) Recent development in the fabrication of metal matrix-particulate composites using powder metallurgy techniques. *J Mater Sci* 29:999–2007
6. Surappa MK (2003) Aluminium matrix composites: challenges and opportunities. In: *Sadhana*, vol 28, Parts 1 & 2. Department of Metallurgy, Indian Institute of Science, Bangalore, pp 319–334
7. Babalola PO, Bolu CA, Odunfa KM (2014) Development of aluminium matrix composites. *Int J Eng Technol Res* 2:1–11
8. Kadolkar PB, Watkins TR, De Hosson JTM, Kooi BJ, Dahotre NB (2007) State of residual stress in laser-deposited ceramic composite coatings on aluminum alloys. *Acta Mater* 55:1203
9. Vreeling JA, Ocelík V, Hamstra GA, Pei YT, De Hosson JTM (2000) In-situ microscopy investigation of failure mechanisms in Al/SiC<sub>p</sub> metal matrix composite produced by laser embedding. *Scripta Mater* 42:589
10. Anandkumar R, Almeida A, Colaço R, Vilar R, Ocelik V, De Hosson JTM (2007) Microstructure and wear studies of laser clad Al-Si/SiC<sub>(p)</sub> composite coatings. *Surf Coat Technol* 201:9497
11. Torres B, Lieblich M, Ibáñez J, García-Escorial A (2002) Mechanical properties of some PM aluminide and silicide reinforced 2124 aluminium matrix composites. *Scripta Mater* 47:45